JOURNAL OF CATALYSIS **162,** 20–30 (1996)
ARTICLE NO. 0256

Effect of Surface Oxidation of the Support on the Thiophene Hydrodesulfurization Activity of Mo, Ni, and NiMo Catalysts Supported on Activated Carbon

A. Calafat,*,†,[1] J. Laine,* A. López-Agudo,† and J. M. Palacios†

*Lab. Fisicoquímica de Superficies, Centro de Química, Instituto Venezolano de Investigaciones Científicas, Apartado 21827, Caracas 1020A, Venezuela; and †Instituto de Catálisis y Petroleoquímica, Consejo Superior de Investigaciones Científicas, Campus Universidad Autónoma, Cantoblanco, 28049 Madrid, Spain

Received July 21, 1995; revised April 3, 1996; accepted April 10, 1996

The present investigation attempts to provide a better understanding of the influence of the nature of the carbon support on the HDS activity of Mo, Ni, and NiMo catalysts. For this purpose a high purity activated carbon was subjected to oxidative treatments with HNO_3 to modify its surface properties. NiMo catalysts supported on the resulting activated carbons were prepared and characterized by TPR, XRD, and SEM–EDX, and their activity for HDS of thiophene at 30 bars and 375°C was evaluated. The results obtained showed that oxidation of the carbon surface does not affect the HDS activity and other characteristics of the supported Mo phase. In contrast, the HDS activity of the Ni catalysts is enhanced by acid treatments of the carbon support. In this case, introduction of oxygen-containing functional groups ($O_{(s)}$) leads to a strong interaction of $O_{(s)}$–Ni during impregnation, which becomes essential to achieving and preserving high nickel dispersion. This effect on Ni dispersion is also reflected on the HDS activity of the bimetallic NiMo/C catalysts. The synergistic effect of the bimetallic catalysts is observed only when oxygen functional groups are present on the carbon surface, which are necessary for a good HDS activity, mainly because they enhance Ni–Mo interactions that produce the highly active Ni–Mo–S phase. A $NiMoO_4$-like phase formed during impregnation seems to be the precursor for the active sulfide phase over the present NiMo/C catalysts.

INTRODUCTION

One growing area in hydrotreatment catalysis is the study of carbon-supported sulfide catalysts, since they exhibit remarkable properties if compared with alumina-based catalysts (1–8). It is now well documented that, in addition to showing improved coking resistance (9, 10), carbon-supported CoMo and NiMo sulfides are more active hydrodesulfurization (HDS) catalysts than the corresponding alumina-supported sulfides (1–7).

While the relatively high HDS activity of carbon-supported catalysts seems to be well understood (2–4), the frequent activity discrepancies reported for catalysts supported on what are supposed to be similar carbons are difficult to predict and understand (11). The origin of these discrepancies seems to lie in the chemical properties of carbon, which are influenced by the nature and quantity of the surface oxygen functional groups (12, 13). Thus, it is the metal precursor/support interaction during support impregnation that requires special attention. Although there have been several attempts to relate the surface properties of the carbon support to the different HDS activities, an understanding of the metal precursor/carbon interactions is not comprehensive. For example, Martín-Gullón *et al.* (14) have described the role of oxygen surface groups as negative while Vissers *et al.* (15) found an increase in activity when a carbon black support was treated to increase the number of oxygen surface groups. In recent studies (11, 16), it was concluded that the extent of adsorption of Mo can be tailored by oxidative and/or thermal treatment of the support, but, in particular, it was concluded that it is not sufficient to create adsorption sites on the support surface: these must also be made accessible to the metal precursor and preserved during catalyst activation.

Within the above scope, the purpose of the present communication is to gain more insight on the effect of the nature of the carbon surface on the HDS reaction over carbon-supported catalysts. The focus is on one support, a high surface area–low ash commercial activated carbon (Merck), in which the surface properties were modified by treatment with different HNO_3 solutions. In contrast with other work (11, 14, 16), we deal not only with molybdenum catalysts but also with Ni and Ni-promoted Mo catalysts, since these effects have not been extensively studied in these mixed metal catalysts.

EXPERIMENTAL PROCEDURE

Catalyst Preparation

A high purity activated carbon (Merck, 917 $m^2 \cdot g^{-1}$, 1 wt% ash) was oxidized by treating it with different

[1] E-mail address: acalafat@quimica.ivic.ve.

0021-9517/96 $18.00

concentrations (0.0, 0.5, 1.0, and 6.0 *M*) of boiling HNO_3 for 8 h, followed by extensive washing with distilled water. The resulting supports (denoted as C-0, C-0.5, C-1, and C-6) were impregnated (incipient wetness impregnation) with ammonium heptamolybdate and/or nickel nitrate solutions. The bimetallic catalysts were first impregnated with molybdenum. The impregnated samples were dried in air at 110°C overnight. The nominal compositions of the catalysts were 5 wt% NiO for the Ni/C samples, 10 wt% MoO_3 for the Mo/C samples, and 3 wt% NiO and 10 wt% MoO_3 for the bimetallic catalysts. Note that these oxides are probably not present, but this convention is followed for consistency with previous work (8, 17). Also note that the catalyst notation for oxidic, dried samples is based on the metal phase (Mo, Ni, or NiMo) followed by the support designation, i.e., Mo/C-6. When the catalysts are sulfided (S) is added to the notation or it is indicated that they are sulfided.

Catalyst Characterization

The surface properties of the original Merck activated carbon and its oxidized derivatives were determined by N_2 adsorption at 77 K using a Micromeritic ASAP 2000 apparatus. The acid site concentration and the acid strength were measured by titrating a suspension of the activated carbon in acetonitrile with *n*-butylamine (n-$C_4H_9NH_2$) 0.1 *N* using a CRISON-MicropH 2001 pH meter.

Temperature programmed reduction (TPR) analyses of the impregnated metal precursors and of the sulfided catalysts were carried out using an apparatus consisting of a gas flow system connected to a thermal conductivity cell to follow changes in the composition of the reducing gas (15 vol% of H_2 in N_2). The samples (0.020 g) were placed into a U-shaped reactor and heated at a constant rate of $20°C \cdot min^{-1}$. The water produced was removed with a liquid nitrogen trap at the reactor outlet. Thus, the observed signals were related only to hydrogen consumption. Peak fitting and peak area calculation were performed using software (shareware GOOGLY, courtesy of Dr. Andy Proctor, Univ. of Pittsburgh), and hydrogen consumption was calibrated by means of known quantities of V_2O_5. Catalysts were sulfided *ex situ* in the TPR U-shape reactor using a mixture of H_2S and H_2 (1/10) for 2 h at 400°C. Before the analysis, the reactor was cooled in He to room temperature and then transferred to the TPR flow system.

X-ray diffraction (XRD) powder patterns of the sulfided catalysts were obtained with Ni-filtered Cu$K\alpha$ radiation using a Seifert 3000 P diffractometer. Catalysts were sulfided *ex situ* using the conditions described above and kept in isoctane at 3°C. All XRD analyses were done 12 h after presulfidation.

Scanning electron microscopy with simultaneous energy dispersive X-ray analysis (SEM–EDX) of the sulfided catalysts was done using an ISI-DS-130 electron microscope equipped with a Si/Li detector and a Kevex 800 processor. Catalysts were sulfided *ex situ* as done for TPR and XRD analysis and kept in isoctane at 3°C. Prior to the analysis, the samples were ground, pressed into wafers, and re-covered with a graphite film.

Catalytic Measurements

The thiophene hydrodesulfurization activity measurements were carried out in a fixed-bed-type reactor connected to a flow system at 30 bar and 375°C. Catalyst samples (0.20 g) were sulfided *in situ* by a mixture of H_2S/H_2 (1/10) at 400°C for 2 h. A solution of 17 wt% thiophene in cyclohexane was introduced into the reaction system by means of a liquid pump at a rate of $12\ ml \cdot h^{-1}$. The reaction products were collected at the end of the reactor and analyzed by gas chromatography.

Conversions measured under steady state conditions (after 2–3 h of reaction) were used to calculate the intrinsic HDS activity per atom of Me [QTOF = quasi turnover frequency, expressed in moles of thiophene converted per atom of *Me* (*Me* = Ni, Mo, or Ni + Mo) per square nanometer support surface area per second].

RESULTS

Surface Area and Acidity of the Supports

Table 1 shows the results obtained from N_2 adsorption analyses and potentiometric titration of the Merck activated carbon and its acid-treated derivatives. Changes in the porosity of the support are observed as the acid concentration of the treatment solution increases. The BET surface area and micropore volume of the activated carbon C-6 are almost 75% of the values obtained for the C-0 sample. Since some destruction of the porosity of the original activated carbon is found when treated with HNO_3, the thiophene hydrodesulfurization activities of the different catalysts have been normalized by the surface area of the different supports used (see below).

The oxidation of the activated carbon surface as a consequence of the treatments with HNO_3 is evident from the acidity results reported in Table 1. For example, the acidity

TABLE 1

Characterization of the Activated Carbon Treated with HNO_3

Activated carbon	C-0	C-0.5	C-1	C-6
HNO_3 treatment	0 M	0.5 M	1 M	6 M
BET surface area, $m^2 \cdot g^{-1}$	917	880	812	710
Micropore volume, $cc \cdot g^{-1}$	0.293	0.281	0.243	0.207
Acidity, meq n-$C_4H_9NH_2$ (0.1 *N*) $\cdot g^{-1}$	1.7	1.8	2.1	3.6
Acid strength, E_0 (mV)[a]	−55 (w)	−6 (w)	203 (vs)	200 (vs)

[a] Initial electrode potential; w = weak, vs = very strong.

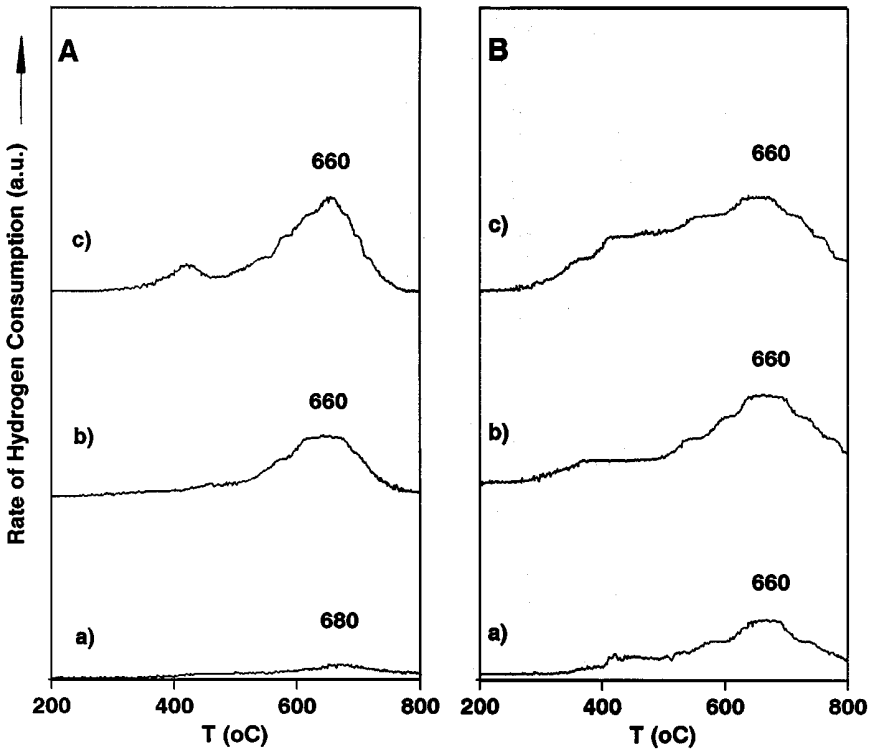

FIG. 1. TPR profiles of (A) nonsulfided and (B) sulfided Merck activated carbon supports: (a) C-0, (b) C-1, (c) C-6.

of the C-6 is twice that observed for the C-0. A considerable increase in the acid strength of the activated carbon surfaces is also observed as the concentration of the acid solution increases.

Temperature Programmed Reduction (TPR)

Activated carbon. TPR profiles of the nonimpregnated supports (Fig. 1A) present a broad band at about 660°C attributed to surface oxygen complexes (18, 19). Note that the intensity of this peak clearly increases with the strength of the oxidation of the activated carbon surface. When the supports are sulfided, their reduction temperatures are similar to those of the nonsulfided samples (Fig. 1B). The intensity of the peak also increases with the strength of acid treatment used. Therefore, TPR data lead us to conclude that the activated carbon used is actually oxidized by the present nitric-acid treatments.

Mo/C catalysts. The TPR profiles of the Mo precursor impregnated on the Merck activated carbon and its derivatives are shown in Fig. 2. All profiles are dominated by a peak with a maximum positioned at similar temperatures, at 580–590°C. For the Mo/C-1 and Mo/C-6 catalysts, a shoulder near 660°C is also evident (Fig. 2A). This last signal could be assigned to the reduction of the carbon support, as its reduction temperature and H_2 consumption are similar to those observed for the nonimpregnated support (Table 2). From Table 2, it is observed that the H_2 consumption related to the first reduction peak (580–590°C) is practically independent of the acid treatment of the Merck activated carbon, indicating that oxidation of the support does not significantly affect the reducibility of the Mo precursor impregnated on the activated carbon.

TPR profiles of the sulfided Mo/C samples also show two reduction peaks (Fig. 2B). From the *r* values showed in Table 2, the peak at 660°C could be clearly assigned to reduction of the bare support. The first peak (450–440°C), due to the reduction of a sulfided Mo species, shifts slightly to lower temperatures when the support is treated with HNO_3. However, the maximum shift is only around 10°C, and it is not clear whether a more reactive sulfided Mo phase is obtained when the carbon surface is oxidized. The amount of H_2 consumption related to this signal seems to increase slightly with the degree of oxidation of the carbon surface (Table 2), but the maximum variation is ca. 10% which is not very significant. Therefore, this suggests that sulfidation of Mo is not strongly affected by support oxidation.

Ni/C catalysts. TPR of the impregnated Ni precursor (Fig. 3A) shows three peaks, at about 390, 450, and 660°C. The second reduction peak, at about 450°C, appears near the reduction temperature of bulk nickel oxide (Fig. 3A.d), suggesting that Ni could be present in an oxide-type phase. The first reduction peak, at about 390°C, corresponds to a phase which is even easier to reduce. This TPR signal could be assigned to reduction either of nickel nitrate species or of

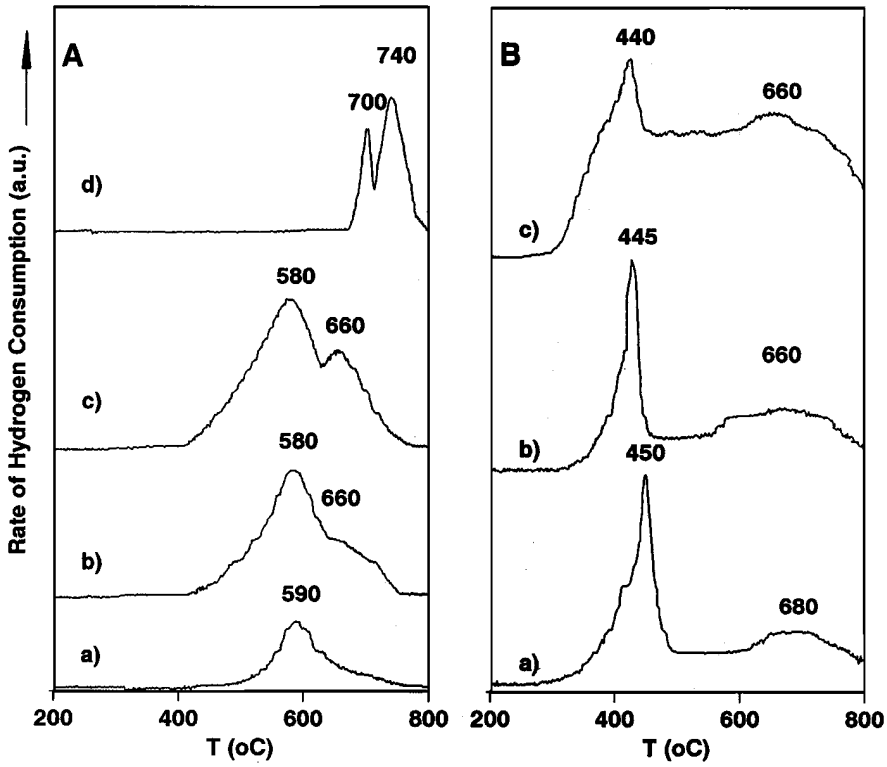

FIG. 2. TPR profiles of (A) impregnated molybdenum heptamolybdate and (B) sulfided Mo on acid treated activated carbons: (a) C-0, (b) C-1, (c) C-6, and (d) bulk MoO_3.

another nickel oxide-type phase. The presence of two well distinguishable oxide phases could be related to a varying degree of interaction between these nickel phases and the surface functional groups of the activated carbon.

The broad, high temperature reduction signal (660°C) observed in the TPR of the Ni/C samples (Fig. 3A) could be assigned to reduction of the carbon support. However, the consumption of hydrogen due to this reduction is notably higher than that observed for the nonimpregnated support, especially for the Ni/C-0 sample (Table 3). Also note that, for this catalyst, the hydrogen consumption due to the first peak (Ni reduction) is significantly lower than for the Ni/C-1 and Ni/C-6 samples. Since all the catalysts have the same Ni loading, the high temperature peak could be assigned not only to reduction of the carbon support but also to Ni reduction. The presence of a high-temperature reduction peak could be related either to a Ni phase in strong interaction with the carbon matrix of the support, which could

TABLE 2

Hydrogen Consumption in TPR of Mo (10 wt%) Supported on Acid Treated Activated Carbons

		Reduction region				
		400–500°C	500–600°C	600–700°C		
Catalyst	Amount of Mo (mmol/g cat)	H_2 (mmol/g cat)	H_2 (mmol/g cat)	H_2	H_2 (supp.)[a] (mmol/g cat)	r^b
Mo/C-0	0.69		1.79	—	0.004	—
Mo/C-1	0.69		2.15	1.03	1.08	0.95
Mo/C-6	0.69		2.00	1.35	1.44	0.94
Mo/C-0 (S)[c]	0.69	1.73		0.78	0.89	0.88
Mo/C-1 (S)	0.69	1.85		0.87	0.95	0.92
Mo/C-6 (S)	0.69	1.93		1.66	1.43	1.16

[a] H_2 (supp.): H_2 consumption due to the non-impregnated support.
[b] $r = H_2/H_2$ (supp.).
[c] (S): sulfided catalysts.

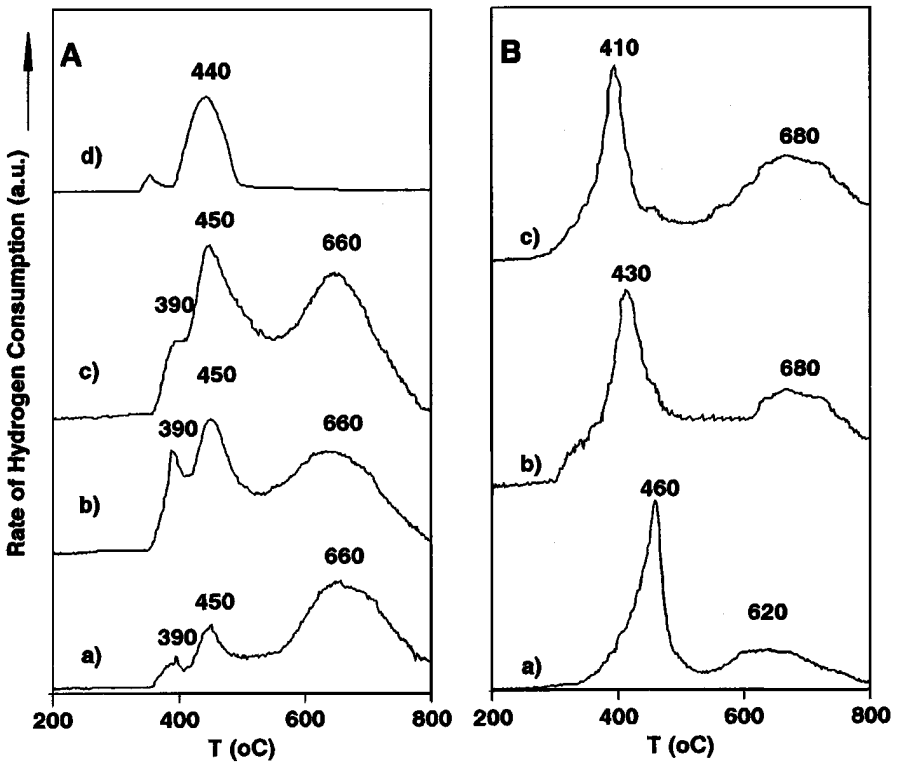

FIG. 3. TPR profiles of (A) impregnated nickel nitrate and (B) sulfided Ni on acid treated activated carbons: (a) C-0, (b) C-1, (c) C-6, and (d) bulk NiO.

produce a refractory Ni phase during TPR analysis, or to different reduction kinetics followed by Ni oxide particles residing in different pores of the activated carbon. Water produced during reduction generally inhibits further reduction when it is retained by the material in the vicinity of the reducible phase (20). It is possible that the micropores retain water more strongly due to special electric field effects, thus making Ni adsorption in the microporosity much stronger than in the remainder of the porous structure. This would mean, on the other hand, that Ni can penetrate the micropores while Mo cannot because such an effect is not observed in Mo catalysts. The relation between low- or high-temperature reduction peaks and different pore sizes has recently been studied in detail (21, 22).

Figure 3A and Table 3 clearly show that oxidation of the activated carbon increases the amount of reducible nickel oxide phases on the catalyst surface. As the acid concentration of the treatment solution increases, H_2 consumption

TABLE 3

Hydrogen Consumption in TPR of Ni (5 wt%) Supported on Acid Treated Activated Carbons

		Reduction region				
		300–400°C	400–500°C	500–700°C		
Catalyst	Amount of Ni (mmol/g cat)	H_2 (mmol/g cat)	H_2 (mmol/g cat)	H_2	H_2 (supp.)[a] (mmol/g cat)	r[b]
Ni/C-0	0.67	0.02	0.04	0.65	0.004	163
Ni/C-1	0.67	0.13	0.36	1.26	1.08	1.17
Ni/C-6	0.67	0.08	0.47	1.48	1.44	1.03
Ni/C-0 (S)[c]	0.67		0.87	0.70	0.89	0.79
Ni/C-1 (S)	0.67		0.93	1.08	0.95	1.14
Ni/C-6 (S)	0.67		0.85	1.37	1.43	0.96

[a] H_2 (supp.): H_2 consumption due to the non-impregnated support.
[b] $r = H_2/H_2$ (supp.).
[c] (S): sulfided catalysts.

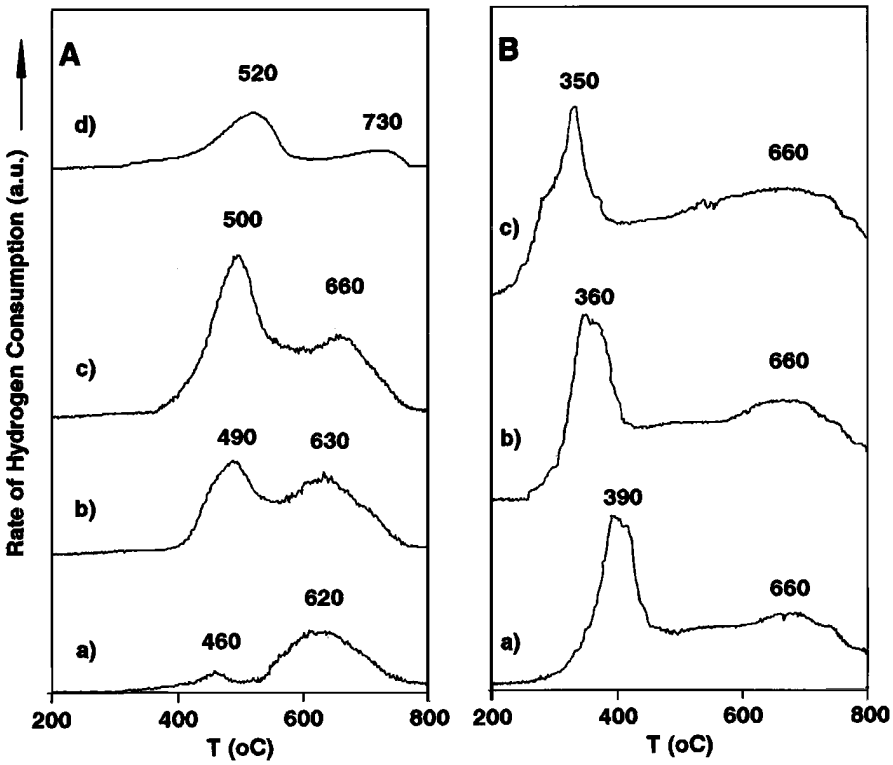

FIG. 4. TPR profiles of (A) impregnated molybdenum heptamolybdate and nickel nitrate, and (B) sulfided NiMo on acid treated activated carbons: (a) C-0, (b) C-1, (c) C-6, and (d) bulk $NiMoO_4 \cdot xH_2O$.

increases due to both the 390 and the 450°C reduction peaks, while that due to the 660°C signal decreases (Table 3, last column). Note that for Ni/C-6, the ratio $r = H_2/H_2$ (supp.) is close to 1, which leads us to assign the high temperature peak only to reduction of the carbon support. Another interesting observation in Table 3 is that the hydrogen consumption due to the 450°C reduction peak increases considerably compared with that for the lower temperature peak when the carbon support is treated with the 6.0 *M* nitric acid solution. It should be expected that a NiO phase in a bound form, or as a surface compound on the carbon, is being favored as the concentration of surface oxygen functional groups increases due to oxidation of the activated carbon.

TPR profiles of the sulfided Ni/C catalysts show two reduction peaks at 410–460 and 660°C (Fig. 3B). As for the sulfided Mo/C catalysts, the peak at 660°C could be assigned to reduction of the sulfided support (Table 3, last column). The first peak at 410–460°C, therefore, could be assigned to reduction of sulfided Ni. As with the Mo/C samples, the amount of H_2 consumed reflected in the peak at lower temperature is independent of the carbon surface oxidation. On the other hand, a shift of about 50°C to lower temperatures is clearly observed for this signal when the activated carbon is more oxidized, showing that the treatment of the support favors the formation of a more easily reducible sulfided Ni phase.

NiMo/C catalysts. Figure 4 shows the TPR profiles of the Ni–Mo precursors impregnated on Merck activated carbon and its derivatives. Two reduction peaks at 460–500°C and 620–660°C can be discerned. For the NiMo/C-1 and NiMo/C-6, the peak at 620–660°C could be related only to reduction of the support (Table 4, last column). For the NiMo/C-0 sample, due to the high *r* value observed (Table 4), this signal could also be assigned to reduction of Mo species (Fig. 4A.a). This is based on the observation that in the Mo/C samples (Fig. 2A) reduction of Mo species takes place at about 590°C and partially overlaps with that of the support. On the other hand, the peak at 460°C observed in this catalyst could be assigned to reduction of a Ni oxidic phase, similar to that proposed for the Ni/C samples.

From Fig. 4, it is clear that oxidation of the activated carbon surface affects the TPR profiles of NiMo/C samples. The peak at 460°C of the NiMo/C-0 catalyst shifts to higher temperatures as the support is being oxidized. Also, H_2 consumption (see Table 4) due to the band at a lower temperature increases considerably as the support is treated with nitric acid, while that due to the 620–660°C reduction peak decreases significantly (Fig. 4A, Table 4). Furthermore, note that for the NiMo/C-1 and NiMo/C-6 catalysts, the *r* value is close to one, indicating that reduction of all the impregnated Ni and Mo occurred at 500°C. When the reduction profiles of these samples are compared with that obtained for bulk commercial $NiMoO_4 \cdot xH_2O$ (Fig. 4A.d) the similarity

TABLE 4

Hydrogen Consumption in TPR of NiMo (3/10) Supported on Acid Treated Activated Carbons

Catalyst	Amount of Ni + Mo (mmol/g cat)	Reduction region				
		300–400°C H_2 (mmol/g cat)	400–500°C H_2 (mmol/g cat)	500–700°C		
				H_2	H_2 (supp.)[a] (mmol/g cat)	r[b]
NiMo/C-0	1.09		0.02	2.07	0.004	518
NiMo/C-1	1.09		1.99	1.22	1.08	1.13
NiMo/C-6	1.09		2.57	1.38	1.44	0.96
NiMo/C-0 (S)[c]	1.09	2.14		0.97	0.89	1.09
NiMo/C-1 (S)	1.09	2.20		1.11	0.95	1.17
NiMo/C-6 (S)	1.09	2.14		1.47	1.43	1.03

[a] H_2 (supp.): H_2 consumption due to the non-impregnated support.
[b] $r = H_2/H_2$ (supp.).
[c] (S): sulfided catalysts.

observed could be suggesting the presence of a mixed oxide phase. Therefore, these results lead us to propose that the peak observed in the TPR of the NiMo/C-1 and NiMo/C-6 samples comes from the reduction of a nickel molybdate-type phase formed when both metal compounds are impregnated on an oxidized activated carbon surface.

The TPR profiles of sulfided NiMo/C catalysts show two reduction peaks at 350–390 and 660°C (Fig. 4B). Comparison with the TPR profiles of the sulfided supports (Fig. 1B and Table 4, last column) shows that the second peak is unambiguously due to reduction of the sulfided support. The first peak, which shifts to temperatures about 40°C lower as the activated carbon is oxidized, may be assigned to reduction of sulfided Ni and Mo phases. As for the Ni/C catalysts, this result indicates that the acid treatment of the support favors the formation of a more reactive sulfided NiMo phase. On the other hand, for the sulfided NiMo/C-6 catalyst (Fig. 4B.c), as we proposed the formation of a $NiMoO_4$-type phase over the acid-treated supports, the 350°C peak in this sample should come from the reduction of the sulfided molybdate-type phase. Indeed, Brito *et al.* (23) have carried out TPR analyses of bulk sulfided $NiMoO_4$ phases which resemble the spectrum observed here for sulfided NiMo/C-6.

X-Ray Diffraction (XRD)

XRD patterns of the sulfided Mo/C catalysts are shown in Fig. 5A. Although the main diffraction peak of MoS_2 ($2\theta = 14°$) could be masked by the activated carbon background, no complementary signal for this compound is found in any of the sulfided catalysts studied. This result seems to indicate that a well dispersed sulfided Mo phase is obtained over activated carbon independent of the degree of surface oxidation.

Diffraction peaks assigned to nickel sulfide phases are clearly observed in the XRD pattern of the sulfided Ni/C-0 catalyst (Fig. 5B.a). Such diffraction peaks, however, are not distinguished in the patterns of the Ni/C-1 and Ni/C-6 catalysts (Fig. 5B, b and c.) The sulfide phases detected seem to be Ni_3S_2 and NiS. This result is unexpected since the thermodynamically stable Ni sulfide in typical HDS conditions is Ni_3S_2 (24). For the present catalysts, the sulfided carbon support is probably stabilizing other Ni sulfide phases. Consistently, a NiS millerite-type phase has been proposed in NiMo/C catalysts as an active phase for HDS (25). In Ni/C catalysts, the sulfided carbon support can act as a sulfur sink to maintain this active Ni phase (8).

An important result here is that the sharp lines and intensities observed show that aggregation of these nickel phases to form large crystals takes place over the nonoxidized activated carbon. When the support is treated by solutions of nitric acid, the diffraction lines are no longer observed, indicating that oxidation of the activated carbon surface may enhance nickel dispersion.

Very similar results are obtained for the sulfided NiMo/C catalysts (Fig. 5C). Evidence of Ni_3S_2 and NiS is also found on the nonoxidized activated carbon (Fig. 5C, a). The diffraction lines for the sulfided nickel phase are, however, not observed in the acid-treated activated carbons (Fig. 5C, b and c). As for the Mo/C catalysts, no peaks due to MoS_2 are found in any of the catalysts studied. These results seem to corroborate that dispersion of the sulfided Ni phase is clearly favored by the oxidation of the support.

Scanning Electron Microscopy–Energy Dispersive X-Ray Analysis (SEM-EDX)

The Mo$L\alpha$ and Ni$K\alpha$ SEM–EDX line profiles of the sulfided Mo/C, Ni/C, and NiMo/C catalysts are shown in Fig. 6. The Mo$L\alpha$ EDX line profiles of the sulfided Mo/C catalysts show that Mo is homogeneously distributed throughout the particle, disregarding the nature of the support.

For Ni supported samples, however, the characteristics of the activated carbon surface affect the distribution of

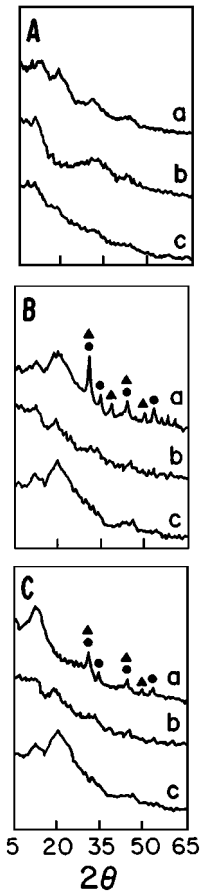

FIG. 5. XRD powder patterns of sulfided Mo/C (A), Ni/C (B) and NiMo/C (C) catalysts for activated carbon supports: (a) C-0, (b) C-1, (c) C-6; ▲, Ni_3S_2; ●, NiS.

the metal over the support. Note that for the nonoxidized activated carbon (Fig. 6B.a) a nonhomogeneous distribution of Ni is obtained, which becomes more homogeneous as the support surface is oxidized (Fig. 6B, b and c). These changes seem to indicate that the functionality of the activated carbon surface affects the dispersion of the Ni, which is enhanced when the concentration of oxygen on the support surface is increased by acid treatment. The results from Fig. 6 seem to corroborate those obtained by XRD analysis, where more crystalline sulfided Ni phases are obtained for the untreated activated carbon.

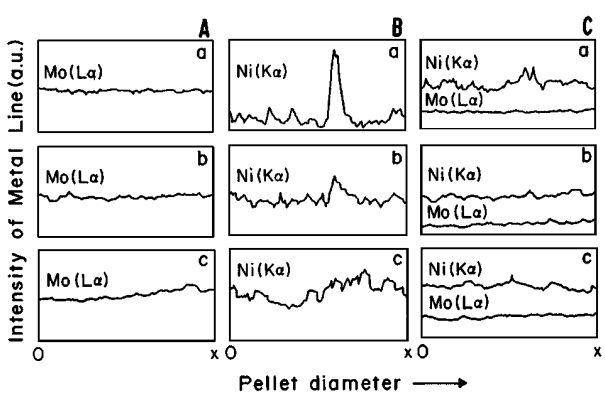

FIG. 6. SEM-EDX line profiles of sulfided Mo/C, Ni/C, and NiMo/C catalysts for activated carbon supports: (a) C-0, (b) C-1, (c) C-6.

Similar results are observed for the NiMo/C catalysts. Homogeneously dispersed Mo is found over all of the supports studied, while distribution of Ni strongly depends on the oxidation of the support surface.

Thiophene Hydrodesulfurization Activity

The results of thiophene HDS activity (Table 5) show that surface oxidation of the Merck activated carbon does not affect the intrinsic catalytic activity (QTOF) of the Mo/C catalysts. This result agrees with that reported by Solar *et al*. (11) where no evidence of a clear correlation between the surface chemical properties of the support and HDS activity was found for Mo/C catalysts prepared by incipient wetness impregnation with ammonium heptamolybdate.

On the other hand, the acid treatment of Merck activated carbon does affect the catalytic behavior of Ni/C samples: the HDS activity is enhanced when the original support is oxidized with HNO_3. Thus, the QTOF value of the C-6 supported catalyst is almost four times higher than that obtained when using the C-0 activated carbon. Furthermore, note that the HDS activity of the Ni/C-6 catalyst is similar to that obtained for the Mo/C-6 catalyst.

Regarding the NiMo/C catalysts, Table 5 shows that the correlation between the surface properties of the support and the HDS activity of NiMo/C catalysts is similar to that of the Ni/C samples: the QTOF increases when the surface carbon is more oxidized. From the results in Table 5, it is

TABLE 5

Thiophene HDS Activity of Mo, Ni, and NiMo Supported on Different HNO_3 Treated Activated Carbons[a]

Catalyst	HNO_3 Treatement	QTOF ($\times 10^4$)[b]
Mo/C-0	0 *M*	52
Mo/C-0.5	0.5 *M*	53
Mo/C-1	1 *M*	47
Mo/C-6	6 *M*	57
Ni/C-0	0 *M*	17
Ni/C-0.5	0.5 *M*	27
Ni/C-1	1 *M*	43
Ni/C-6	6 *M*	63
NiMo/C-0	0 *M*	44
NiMo/C-0.5	0.5 *M*	57
NiMo/C-1	1 *M*	265
NiMo/C-6	6 *M*	332

[a] Reaction conditions: $T = 375°C$; $P = 30$ bar; $W/F = 8.5\ g_{CAT} \cdot h \cdot mol^{-1}$.

[b] Intrinsic catalytic activity, [(mmol thiophene converted)/(total atoms Me)] $\cdot\ nm^2 \cdot\ s^{-1}$, where Me = Mo, Ni, Mo + Ni.

clear that the effect of the carbon surface oxidation on the HDS activity of Ni/C catalysts is paralleled by the promoting role of Ni in NiMo/C catalysts. Note that when using C-0 and C-0.5 supports, the activities of NiMo samples are similar to those obtained for Mo catalysts, while for C-1 and C-6 the QTOF values of NiMo catalysts are almost six times the corresponding values for Mo samples. This finding contrasts with that of Bowens *et al*. (26) for carbon-supported NiMo catalysts, where a strong promotion effect takes place on a nonoxidized carbon. Probably, this difference in the Ni promotion effect for nonoxidized supports is caused by differences in the type of activated carbon used. For example, Bowens *et al*. used an activated carbon (Norit, RX3 Extra) which is washed with HCl by the manufacturer to reduce the impurity content. Thus, it is possible that the oxidation degree of this activated carbon, due to the acid treatment, could not be comparable with that of the nonoxidized activated carbon used for the present work.

DISCUSSION

No evidence of a correlation between the oxidized state of the carbon support and HDS activity was found for the Mo/C catalysts. Moreover, the results obtained by TPR, XRD, and SEM–EDX analysis show that oxidation of the support does not affect the characteristics of the Mo phase obtained over the activated carbon, neither during impregnation nor after the sulfidation stage. Independently of the acid treatment of the support, the dispersion of Mo seems to be unaffected. This explains the similar activities observed for the different Mo/C catalysts and suggests either that the oxygen functional groups of the activated carbon are not important as Mo anchoring sites or, if they should be, that they have not been optimally used.

The problem of an insensible Mo to the changes produced on the surface functionality of the carbon support seems to stem from the conflict that exists between active site creation and surface accessibility (11, 16). Oxidation of the carbon surface is the principal vehicle for achieving high Mo dispersion, by introducing oxygen functional groups that serve as anchoring sites for the metal. However, besides enhancing the adsorptive properties of the activated carbon, oxidation renders the support surface negatively charged over a wide range of impregnation pH conditions. The access of molybdenum anions to these sites is, therefore, not favored by repulsive electrostatic forces.

This should be the case for the results observed in the present work. No matter how much the activated carbon surface is oxidized, if the impregnation conditions are not optimal, dispersion of molybdenum could not be improved and activity of the catalysts will be, as can be observed from the present results, insensitive to the kind of carbon support used. One could expect that very low impregnation pH values, when the interactions between the support and the metal precursor are favorable, could be appropriate to achieve high metal dispersion. However, molybdate polymerization seems to preclude the achievement of high catalyst dispersion (16, 27). Also, high initial Mo dispersion may not lead to high activity: final dispersion is also influenced by the thermal stability of the oxygen functional groups on the activated carbon surface (11).

Although Mo is not affected by oxidation of the activated carbon, the HDS activity of the NiMo catalysts is considerably enhanced by acid treatments of the support because of the tremendous effect that the presence of an oxygenated surface has on Ni during catalyst impregnation and, as a consequence, on the species resulting from sulfiding.

As observed from TPR analysis of Ni/C catalysts, introduction of oxygen functional groups ($O_{(s)}$) by treatment of the activated carbon with nitric acid leads to a strong $O_{(s)}$–Ni interaction during impregnation, forming a nickel-oxide-type phase which becomes the preferred one as the support surface is more oxidized. Judging from the results obtained by SEM–EDX and XRD analysis, the formation of this oxide phase is necessary for achieving and preserving, after the sulfidation stage, high nickel dispersion. If the anchoring sites do not exist in an appropriate concentration, as for the untreated activated carbon, a poor distribution of nickel over the support cannot be avoided. When the catalyst is sulfided, the absence of an $O_{(s)}$–Ni interaction leads to the formation of crystalline Ni–S phases, as XRD analysis shows.

Obviously, nickel dispersion is responsible for the high HDS activity of the Ni/C catalysts. Only a well dispersed Ni–S active phase shows high QTOF values, activities that in the present case are comparable with those observed for the Mo/C catalysts. This active Ni–S phase could be small Ni_3S_2 particles dispersed over the carbon support (28, 29) or a NiS millerite-type phase (25). As observed with XRD, these phases tend to agglomerate without $O_{(s)}$–Ni interaction during impregnation, rendering the catalyst less active for HDS.

Ni dispersion also affects the HDS activity of the NiMo/C catalysts. The promoting effect of Ni in the HDS activity of the Mo/C catalysts is only observed when sufficient oxygen functional groups are introduced on the carbon surface by treatments with nitric acid. Note that for the Mo and NiMo catalysts supported on the nonoxidized activated carbons (C-0 and C-0.5), QTOF values are the same, showing that the promoter effect of Ni does not exist in these NiMo catalysts. From our results, the surface of these catalysts could be assumed to be a well-dispersed MoS_2 phase together with agglomerates of nickel sulfides, a situation that should be originated at the impregnation stage. As we mentioned above, the absence of oxygen functionality on these supports seems to preclude the achievement of a well stabilized and dispersed Ni phase that, in the NiMo/C catalysts, may facilitate the synergism of Ni and Mo.

The synergistic effect of Ni and Mo could be envisaged either as remote control effect (30, 31), since the HDS activity seems to be mainly governed by Ni dispersion, or through the promotion of the active Ni–Mo–S phase (25, 29, 32). The experimental results presented here do not allow us to determine which of the two promotion models is operative. Nevertheless, the fact that a $NiMoO_4$-like phase was detected in the nonsulfided NiMo catalysts, as the TPR results suggest, seems to favor the Ni–Mo–S phase explanation. Note that the reduction profile of the NiMo/C-6 is similar to that observed for bulk $NiMoO_4 \cdot xH_2O$, and the TPR analyses of the sulfided catalyst match very well those reported by Brito *et al*. (23) for the sulfided β-$NiMoO_4$. These authors found high thiophene HDS activity for the sulfided molybdates studied, suggesting that phases resembling the β-isomorph could be present in industrial-type NiMo catalysts and could act as convenient precursors of very active sulfided catalysts. In connection with this, Melo *et al*. (33) found a correlation of the amount of "xNiO · MoO_3" in the oxidic precursor with HDS activity of the sulfided catalysts; as previously demonstrated (34), the phase erroneously described as xNiO · MoO_3 · yH_2O was in fact β-$NiMoO_4$. In view of the results presented here, we suggest, therefore, that a $NiMoO_4$-like phase formed during impregnation is the precursor of the Ni–Mo–S phase over the present carbon-supported NiMo catalysts. High Ni dispersion is essential for good HDS activity, mainly because it enhances, during impregnation, the Ni–Mo interactions that produce the $NiMoO_4$-like phase.

CONCLUSIONS

The results obtained show that introduction of surface oxygen groups by acid treatments of the activated carbon affects neither the HDS activity nor the characteristics of the Mo phase obtained over the activated carbon. These results indicate either that the oxygen functional groups are not important as Mo anchoring sites or, if they are, they are not accessible to molybdenum due to the impregnation conditions.

It is concluded, therefore, that an understanding of the nature of the activated carbon surface is the key to achieving good catalytic behavior for Mo HDS catalysts. Oxidation of the support surface to improve metal dispersion is not enough if, in addition, the optimum conditions for catalyst preparation are not achieved, conditions that should be chosen with knowledge of the surface chemistry of the particular carbon support.

On the other hand, the HDS activity of the Ni catalysts is enhanced by acid treatments of the support due to the tremendous effect that the presence of an oxygenated surface has on Ni during catalyst impregnation and catalyst sulfidation. Introduction of oxygen functional groups, $O_{(s)}$, leads to a strong interaction of $O_{(s)}$–Ni during impregnation, forming a nickel-oxide-type phase which becomes essential to achieving and preserving high nickel dispersion. If the anchoring sites do not exist in an appropriate concentration, a poor distribution of nickel over the support cannot be avoided.

Ni dispersion also affects the HDS activity of the NiMo/C catalysts. The promoting effect of Ni in the HDS activity of the Mo/C catalysts is only observed when oxygen functional groups are introduced on the carbon surface. High Ni dispersion is essential for a good HDS activity, mainly because it enhances Ni–Mo interactions that produce, by sulfidation, the active Ni–Mo–S phase. In view of the results presented here, a $NiMoO_4$-like phase which forms during impregnation is proposed as the precursor for the highly HDS active Ni–Mo–S phase over the present carbon-supported NiMo catalysts.

ACKNOWLEDGMENTS

This research was partially supported by Project CE93-0012 DGICYT (Spain). Financial support from the Venezuelan Consejo Nacional de Investigaciones Científicas y Tecnológicas (CONICIT) and the Gran Mariscal de Ayacucho Foundation (Fundayacucho) for a grant to A.C. is gratefully acknowledged. Special thanks to M. P. Borque and M. Toural for their collaboration. This paper is dedicated to the memory of Francisco Severino (l953–l995).

REFERENCES

1. Duchet, J. C., van Oers, E. M., de Beer, V. H. J., and Prins, R., *J. Catal.* **80**, 386 (1983).
2. Vissers, J. P. R., de Beer, V. H. J., and Prins, R., *J. Chem. Soc. Faraday Trans. 1* **83**, 2145 (1987).
3. Vissers, J. P. R., Scheffer, B., de Beer, V. H. J., Moulijn, J. A., and Prins, R., *J. Catal.* **105**, 277 (1987).
4. Scheffer, B., Arnoldy, P., and Moulijn, J. A., *J. Catal.* **112**, 516 (1988).
5. Hillerová, E., and Zdrazil, M., *Catal. Lett.* **8**, 215 (1991).
6. Hillerová, E., Vít, Z., Zdrazil, M., Shkuropat, S. A., Bogdanets, E. N., and Stasrtsev, A. N., *Appl. Catal.* **67**, 231 (1991).
7. Vít, Z., *Catal. Lett.* **13**, 131 (1992).
8. Laine, J., Severino, F., Labady, M., and Gallardo, J., *J. Catal.* **138**, 145 (1992).
9. de Beer, V. H. J., Derbyshire, F. J., Groot, C. K., Prins, R., Scaroni, A. W., and Solar, J. M., *Fuel* **63**, 1095 (1984).
10. Scaroni, A. W., Jenkins, R. G., and Walker, P. L., *Appl. Catal.* **14**, 173 (1985).
11. Solar, J. M., Derbyshire, F. J., de Beer, V. H. J., and Radovic, L. R., *J. Catal.* **129**, 330 (1991).
12. Guerrero-Ruiz, A., Rodríguez-Ramos, I., Rodríguez-Reinoso, F., Moreno-Castilla, C., and López-González, J. D., *Carbon* **26**, 417 (1988).
13. Prado-Burguete, C., Linares-Solano, A., Rodríguez-Reinoso, F., and Salinas-Martínez de Lecea, C., *J. Catal.* **115**, 98 (1989).
14. Martín-Gullón, A., Prado-Burguete, C., Rodríguez-Reinoso, F., and Martos, J., *in* "Proc. of the 20th Biennial Conf. Carbon, Univ. of California, Santa Barbara, June 1991," p. 88.
15. Vissers, J. P. R., Bouwens, S. M. A. M., de Beer, V. H. J., and Prins, R., *Carbon* **25**, 485 (1987).
16. Solar, J. M., León y León, C. A., Osseo-Asare, K., and Radovic, L. R., *Carbon* **28**, 369 (1990).

17. Laine, J., Brito, J . L., and Severino, F., *J. Catal.* **131**, 385 (1991).
18. Laine, J., Calafat, A., and Labady, M., *Carbon* **27**, 191 (1989).
19. Laine, J., Severino, F., and Labady, M., *J. Catal.* **147**, 355 (1994).
20. Arnoldy, P., de Jonge, J. C. M., and Moulijn, J. A., *J. Phys. Chem.* **89**, 4517 (1985).
21. Mile, B., Stirling, D., Zammit, M. A., Lovell, A., and Webb, M., *J. Catal.* **114**, 217 (1988).
22. Afzal, M., Mahmood, F., and Saleem, M., *Carbon* **31**, 757 (1993).
23. Brito, J. F., Barbosa, A. L., Albornoz, A., Severino, F., and Laine, J., *Catal. Lett.* **26**, 329 (1994).
24. McKinley, J. B., *in* "Catalysis" (P. B. Emmet, Ed.), Vol. 5, p. 405. Reinhold, New York, 1957.
25. Bouwens, S. M. A. M., Koningsberger, D. C., de Beer, V. H. J., Louwers, S. P. A., and Prins, R., *Catal. Lett.* **5**, 273 (1990).
26. Bowens, S. M. A. M., Barthe-Zahir, N., de Beer, V. H. J., and Prins, R., *J. Catal.* **131**, 326 (1991).
27. Cruywagen, J. J., and Wet, H. F., *Poyhedron* **7**, 547 (1988).
28. de Beer, V. H. J., Duchet, J. C., and Prins, R., *J. Catal.* **72**, 369 (1981).
29. Louwers, S. P. A., and Prins, R., *J. Catal.* **133**, 94 (1992).
30. Delmon, B., *Catal. Lett.* **22**, 1 (1993).
31. Karroua, M., Centeno, A., Matralis, H. K., Grange, P., and Delmon, B., *Appl. Catal.* **51**, L21 (1989).
32. Topsoe, H., Clausen, B. S., Candia, R., Wivel, C., and Morup, S., *J. Catal.* **68**, 433 (1981).
33. Melo, F. V., Sanz, E., Corma, A., and Mifsud, A., *in* "Studies in Surface Science and Catalysis" (B. Delmon, P. Grange, P. A. Jacobs, and G. Poncelet, Eds.), Vol. 31, p. 557., Elsevier, Amsterdam, 1987.
34. Brito, J. L., and Laine, J., *Appl. Catal.* **72**, L13 (1991).